ADVANCES IN ATMOSPHERIC SCIENCES, VOL. 31, MARCH 2014, 468–479

The Relationship between the El Niño/La Niña Cycle and the Transition Chains of Four Atmospheric Oscillations. Part I: The Four Oscillations

PENG Jingbei*, CHEN Lieting, and ZHANG Qingyun

International Center for Climate and Environment Sciences, Institute of Atmospheric Physics, Chinese Academy of Sciences, Beijing 100029

(Received 1 November 2012; revised17 April 2013; accepted 23 May 2013)

ABSTRACT

The first leading modes of the interannual variations in low-level circulation over the North and South Pacific are the Northern Oscillation (NO) and Southern Oscillation (SO), which are oscillations in sea level pressure anomalies (SLPAs) between the eastern and western Pacific Ocean. The second leading modes are the North Pacific Oscillation (NPO) and the Antarctic Oscillation (AAO), which reflect oscillations between the subtropics and the high and middle latitudes. The transition chains of these four oscillations were investigated using the National Centers for Environmental Prediction–National Center for Atmospheric Research (NCEP–NCAR) reanalysis data. The general pattern of the transition chain between the NO and NPO was from the negative phase of the NO (NO^-) to the positive phase of the NPO (NPO^+), then from NO^+ to NPO^- to NO^-. The whole transition chain took about 4–6 years. The general pattern and period of the transition between the SO and AAO were similar to those between the NO and NPO. In addition, the transition chains between the NO and NPO, and the SO and AAO, were almost simultaneous. The transition chains of the four oscillations were found to be closely connected, with the eastward propagations of SLPAs occurring along both sides of the Equator.

Key words: oscillation, interannual variation

Citation: Peng, J. B., L. T. Chen, and Q. Y. Zhang, 2014: The relationship between the El Niño/La Niña cycle and the transition chains of four atmospheric oscillations. Part I: The four oscillations. *Adv. Atmos. Sci.*, **31**(2), 468–479, doi: 10.1007/s00376-013-2275-0.

1. Introduction

One of the fundamental questions about the nature and prediction of El Niño (EN)/La Niña (LN) is how a cold state turns into a warm state, or vice versa (Wang, 1995). Various hypotheses for the EN/LN cycle have been developed during the last few decades, such as the delayed oscillation model (Suarez and Schopf, 1988), recharge oscillation model (Jin, 1997), and mid-latitude atmospheric variability by producing tropical zonal wind stress anomalies (Li, 1990; Barnett et al., 1999; Pierce et al., 2000). Since Bjerknes (1969) clearly linked the anomalous atmospheric circulation patterns known as the Southern Oscillation (SO) with EN, the connections between atmospheric oscillations and the EN/LN cycle have formed the focus of much research.

In the 1980s, Chen and Zhan (1984) discovered an east–west out-of-phase oscillation in the sea level pressure anomalies (SLPAs) in the Pacific at latitudes symmetric to the SO, with two centers in Manila and at the Ship *N* station (30°N, 140°W) respectively, and named it the Northern Oscillation (NO). Numerical simulation of the climate and diagnostic analyses since confirmed the existence of the NO (Zeng, 1987; Fu and Ye, 1988; Chen and Yan, 1989). As the counterpart of the SO, the NO is also closely connected to EN/LN on both the interannual and interdecadal timescale (Chen, 1982, 1992). During the negative phase of the NO (NO^-), the subtropical high in the North Pacific is weaker than usual, with southwesterly anomalies prevailing over the northeastern Pacific, westerly anomalies over the tropical North Pacific, and warm sea surface temperature anomalies (SSTAs) dominating in the tropical eastern Pacific. Jin and Chen (1992) studied the differences in the relationship between the SO, NO and SSTAs in the Pacific domain. The SO affects SSTAs in the regions of the Peru–Chile current and the south equatorial current, whereas the NO affects those in the regions of the north equatorial current and the equatorial countercurrent. Moreover, the asynchronous variations in the SO and NO lead to different types of EN: the eastern Pacific EN and the Central Pacific EN (Peng et al., 2011).

Recent research has revealed that mid-latitude atmospheric variability might affect tropical SST variability. In the winter of the negative phase of the North Pacific Oscillation (NPO^-) (Montgomery, 1940), the weakened North Pacific Subtropical High leads to warm SSTAs in the tropical and subtropical northwestern Pacific through changes in net

* Corresponding author: PENG Jingbei
Email: pengjingbei@mail.iap.ac.cn

surface heat flux. These persistent SSTAs then force westerly anomalies in the tropical Pacific in the following spring and summer, acting as a forcing of EN variability (Vimont et al., 2001, 2003).

As more comprehensible and more complete data became available, the Antarctic Oscillation (AAO), which is the oscillation between the middle and high latitudes in the Southern Hemisphere, was discovered by Gong and Wang (1999). Results regarding the relationship between the SO and the AAO have been contradictory. Many papers have argued the case for a minimal contemporaneous correlation between the AAO and SO (Gong and Wang, 1999; Schneider and Steig, 2002), while others have reported that negative (positive) AAO phases are dominant during warm (cold) phases of EN/LN (Carvalho et al., 2005).

However, most previous studies have been limited to analyzing the connections between individual oscillations with EN. Wu and Chen (1995) studied the interannual variations of low-level circulation evolution over two full ranges of EN/LN cycles for the period 1980–89. They found that, between the positive phase of the NO (NO^+), corresponding to LN, and NO^-, corresponding to EN, the distributions of circulation anomalies resembled those of the negative/positive phases of the NPO. During each EN/LN cycle, the low-level circulation in the North Pacific experienced a complete transition chain between the NO and NPO, i.e., $NO^- \rightarrow NPO^+ \rightarrow NO^+ \rightarrow NPO^- \rightarrow NO^-$. However, their results were based on a case study.

Thus, whether and how the NO, SO, NPO and AAO (hereafter referred to as "the four oscillations") interrelate, as well as their general relationships with the EN/LN cycle, are unclear. To address this question, we discuss in the present paper: (1) the transition chains of the four oscillations; (2) the relationship between the transition chains and the EN/LN cycle; and (3) a new perspective on prediction of the onset of EN based on the transition chains. The study is composed of five sections in order to examine the transition chains of the four oscillations in detail. Section 2 describes the data and the analysis methods. Section 3 presents the leading patterns of interannual variability of the low-level circulation over the Pacific domain and their resemblances to the four oscillations. Section 4 documents the transition chains of the four oscillations and corresponding low-level circulation evolution. The final section offers a summary of the results and the major findings. Further discussion on the relationship between the transition chains and the EN/LN cycle is provided in Part II of the study (Peng et al., 2013).

2. Data and methods

2.1. *Data and the indices of the four oscillations*

We analyzed monthly sea level pressure (SLP) and wind over 1000 hPa (denoted as $\boldsymbol{V}_{1000}$) from the National Centers for Environmental Prediction–National Center for Atmospheric Research (NCEP–NCAR) reanalysis, which are available on a global 2.5° latitude/longitude grid (Kalnay et al., 1996). The observation-based Southern Oscillation Index (SOI) and Antarctic Oscillation Index (AAOI), provided by the National Oceanic and Atmospheric Administration/Climate Prediction Center, were also used.

Following the definition in Chen and Zhan (1984), the Northern Oscillation Index (NOI) was defined as

$$\mathrm{NOI} = \mathrm{SLP}'_{(25^\circ-37.5^\circ\mathrm{N},147.5^\circ-135^\circ\mathrm{W})} - \mathrm{SLP}'_{(10^\circ-17.5^\circ\mathrm{N},117.5^\circ-122.5^\circ\mathrm{E})},$$

where the superscript $'$ means the normalized area mean. This definition of the NOI is different to that in Schwing et al. (2002), who defined the NOI as the difference in the area mean SLP between the climatological center of the North Pacific High and that near Darwin, Australia. The two areas in this latter definition cross the Equator, whereas the definition we used was limited to the North Pacific.

The original definition of the index of the NPO (NPOI) was defined by the difference in the SLP between Dutch Harbor, Alaska, and Honolulu, Hawaii (Montgomery, 1940). However, owing to the lack of station observations, we used the area mean SLP near the two sites instead of observations and defined the NPOI as

$$\mathrm{NOI} = \mathrm{SLP}'_{(15^\circ-27.5^\circ\mathrm{N},167.5^\circ-147.5^\circ\mathrm{W})} - \mathrm{SLP}'_{(50^\circ-60^\circ\mathrm{N},175^\circ-155^\circ\mathrm{W})}.$$

Apart from the AAOI, all data covered 56 years during the period 1951–2006, and the long-term monthly means were computed over this 56-yr record. The AAOI covered 1979–2006, and its annual cycle was computed over that period.

2.2. *Methods*

We began our study by examining the power spectra of the indices of the four oscillations (Fig. 1). Statistically significant peaks at 5.3, 3.7 and 2.5 years were observed for the NOI and the SOI. Spectral peaks at 5.3 and 3.7 years for the NPOI and a spectral peak at 4.7 years for the AAOI exceeded the 95% confidence level. The significant interannual periods were consistent with previous studies (Rasmusson and Carpenter, 1982; Chen and Zhan, 1984). Based on the spectral analysis, interannual anomalies (3–7 years) were obtained using a second-order Butterworth filter (Li, 1991). The data were normalized before applying a bandpass filter to highlight the variability in the tropics, which is generally weaker than that in the middle and high latitudes.

Next, we applied empirical orthogonal functions (EOFs) to the monthly SLPAs and $\boldsymbol{V}_{1000}$ anomalies (denoted as $\boldsymbol{V}'_{1000}$) to search the leading modes of the low-level circulation over the Pacific basin. A cross-time-lagged correlation analysis and principal oscillation pattern (POP) were applied to examine the connections among the four oscillations and the evolution of interannual SLPAs.

The level of significance of the time-lag correlation was estimated by a Monte Carlo approach (Livezey and Chen, 1983; Shi et al., 1997). For a given time lead, the correlation coefficient was calculated between two filtered random

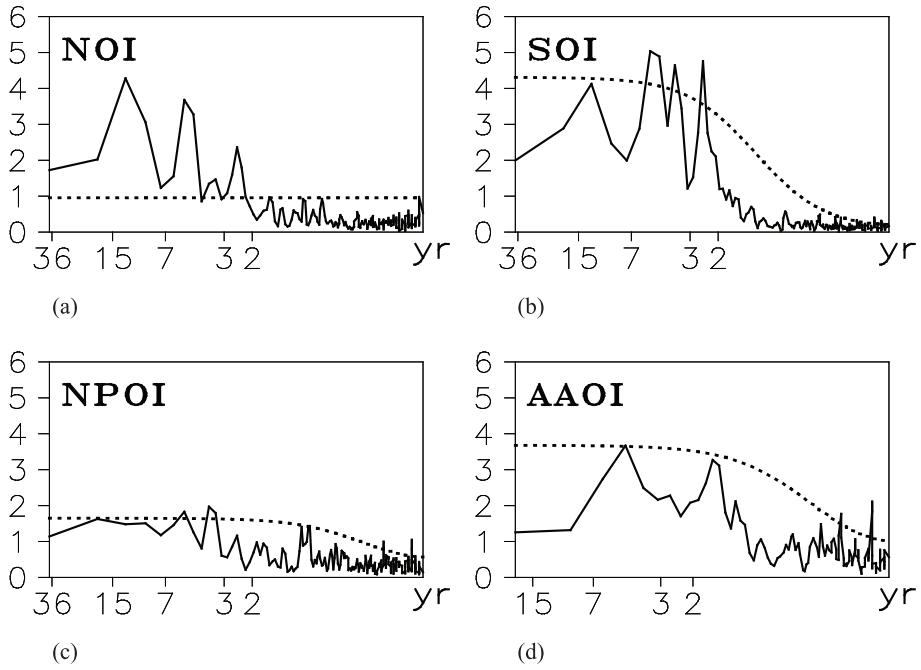

Fig. 1. Power spectra of the indices of (a) NO, (b) SO, (c) NPO and (d) AAO (solid lines). Smooth dashed lines represent the 5% significance level. Units: yr.

series repeatedly. For each lead, 10 000 iterations were performed to develop a null distribution. If the actual correlation coefficient was at or above the 95th percentile of the null distribution, significance at the 5% level was determined.

Phase space analysis was used to study the characteristics of the transition chains of the four oscillations. Phase space is an M-dimensional Euclidean space whose coordinates describe the state of a system (Lorenz, 1963). The state and variation of the system are represented by the phase particle and a trajectory in the space, respectively. In practice, there are many different kinds of orthogonal bases to reconstruct phase space. The EOF basis is one of the best choices because it attempts to account for the maximum variance, and the principal component (PC) time series of each EOF is orthogonal to one another. Wang and Wang (2000) combined EOF and phase space analysis to discuss the evolution of EN/LN. We used the PCs obtained in the EOF analysis of SLPAs to reconstruct the phase space.

3. Examination of the existence of the four oscillations

To examine the existence of the four oscillations, we applied EOF analysis to the interannual variations of SLPAs and $\boldsymbol{V}'_{1000}$ over the Pacific basin (75°S–75°N, 90°E–90°W) during 1951–2006. The first two modes of SLPAs explained 46.27% and 17.74% of the variability, respectively. The first two modes of $\boldsymbol{V}'_{1000}$ explained 22.62% and 11.11% of the variability. The first modes of SLPA and $\boldsymbol{V}'_{1000}$ showed clearly that the four oscillation centers were located both to the north and south of the Equator, reflecting two east–west oscillations in the tropics (Fig. 2, top row), which is consistent with previous work (Fu and Ye, 1988). The second mode of SLPA ($\boldsymbol{V}'_{1000}$) was characterized by two pairs of positive and negative anomaly centers (anticyclonic and cyclonic centers) that reflected the south–north oscillations near the date line over the North and South Pacific Ocean (Fig. 2, bottom row). The spatial structures of the four oscillations resembled the SO, NO, AAO and NPO, respectively, thus providing more evidence for the existence of the four oscillations. Furthermore, the four oscillations were the leading modes of the interannual variations in SLPAs over the Pacific basin.

To examine the relationship between the PCs of SLPAs and the indices of the four oscillations, EOF analysis was applied to the interannual variation in SLPAs over the North and South Pacific, respectively. The first two modes of SLPAs over the North Pacific (0°–60°N, 100°E–80°W) (hereafter referred to as NEOF1 and NEOF2, and their principal components as NPC1 and NPC2) explained 44.65% and 22.22% of the variability, respectively. NEOF1 reflected the east–west out-of-phase oscillation in the tropical North Pacific, which was similar to the NO (Fig. 3, top left). NEOF2 depicted a zonal SLP dipole on either side of 45°N and resembled the NPO (Fig. 3, top right).

In the South Pacific region (80°S–0°, 50°E–80°W), the first two modes (SEOF1 and SEOF2, with principal components SPC1 and SPC2) explained 46.55% and 20.21% of the variability, respectively. The dominant pattern of SEOF1 resembled that of the SO (Fig. 3, bottom left), while SEOF2 reflected the atmospheric oscillation in the middle and high latitudes in the South Pacific (Fig. 3, bottom right), which was similar to the AAO. In fact, the so-called South Pacific region extended to the eastern part of the southern Indian

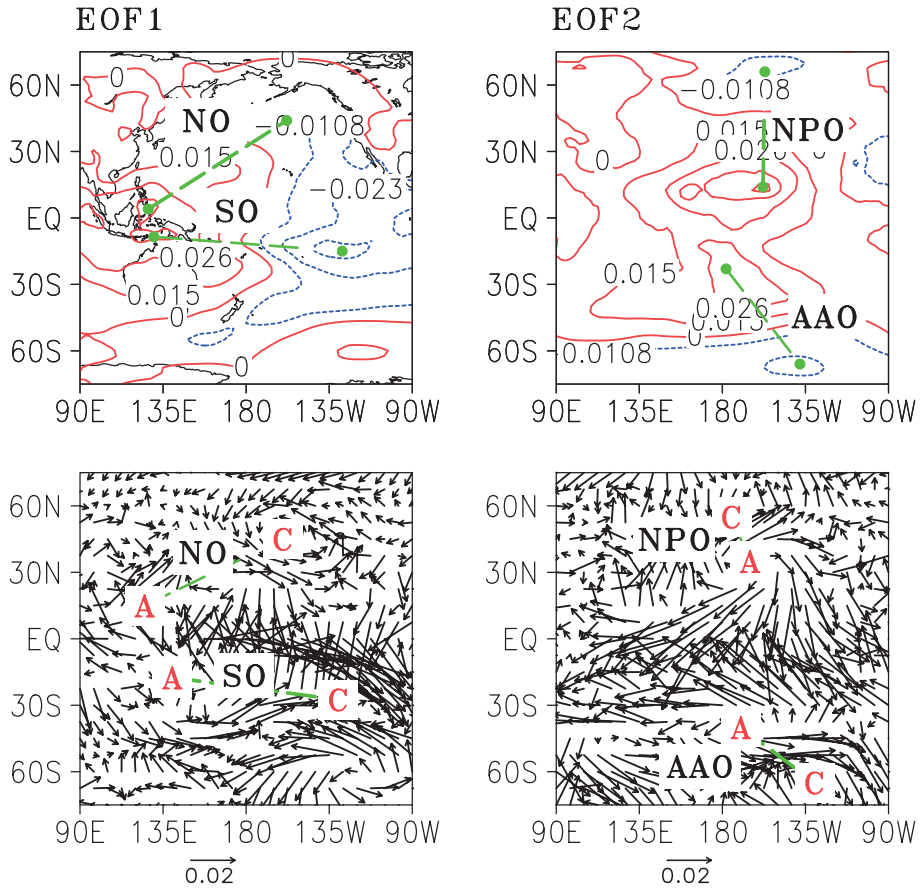

Fig. 2. The first two EOF modes from the interannual variation in SLPAs (top row) and $\boldsymbol{V}'_{1000}$ (bottom row) in the Pacific basin. The green dashed lines denote the four oscillations.

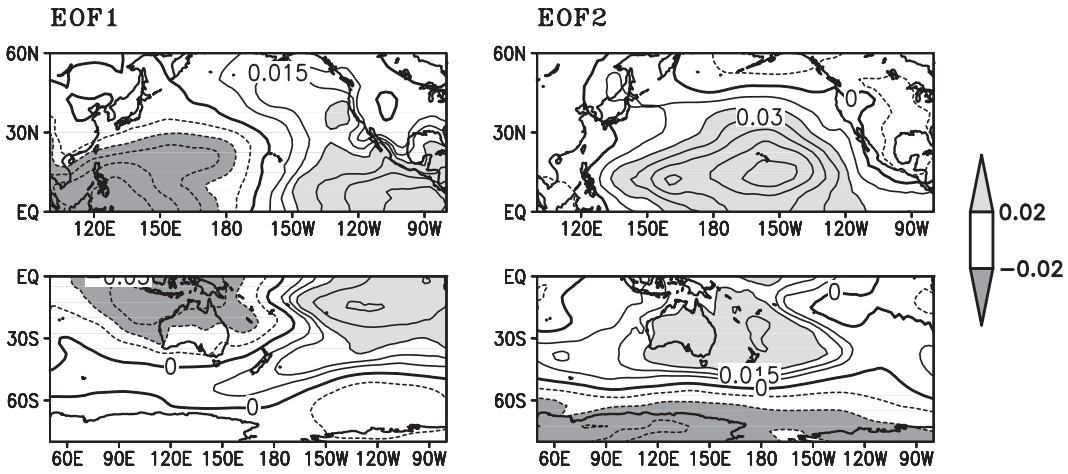

Fig. 3. The first two EOF patterns from the interannual variation in SLPs over the North Pacific (top row) and South Pacific (bottom row).

Ocean to obtain a full image of SEOF1. when we concentrated on the South Pacific (80°S–0°, 105°E–80°W), the first two EOF modes (not shown) were similar to those in Fig. 3. Thus, SEOF1 and SEOF2 were the leading modes of the South Pacific.

We calculated the correlation coefficients of the indices of the four oscillations and the PCs (Table 1), and found that statistically significant relationships existed between the NOI and NPC1, the NPOI and NPC2, the SOI and SPC1, and the AAOI and SPC2. The EOF related to the physical modes through the correlation of the time series and spatial patterns; namely, the NO to NEOF1, the NPO to NEOF2, the SO to SEOF1, and the SEOF2 to part of the AAO in the South Pacific section. Although it is a global oscillation, the major

Table 1. The correlation coefficients between the PCs and interannual variations in the indices of the four oscillations.

	NPC1	NPC2	SPC1	SPC2
NOI	0.86*	0.30	0.82*	−0.14
NPOI	−0.15	0.86*	0.07	0.39
SOI	0.90*	0.24	0.94*	−0.17
AAOI	0.16	0.46	0.30	0.83*

*Significant at the 5% level.

spatial features of the AAO are one prominent action center near 57°S over the Pacific and one of the three out-of-phase centers over the southern Pacific Ocean (Raphael and Holland, 2006; Zhu and Wang, 2010). This may explain the significant correlation coefficient between SPC2 and AAOI. SEOF2 represented most interannual variation of the AAO. Thus, we refer to SEOF2 as the AAO, and use NPC1 and NPC2 (SPC1 and SPC2) to represent the NOI and the NPOI (SOI and AAOI), respectively.

The first two EOFs in the North and South Pacific accounted for nearly two-thirds of the variance of interannual variations in SLPs. Thus, the NO and NPO (SO and AAO) were the leading modes of low-level circulation in the North (South) Pacific.

4. The connections and transition chains of the four oscillations

4.1. *The connections among the four oscillations*

We calculated the lagged correlation between the NOI and SOI, the NPOI and NOI, and the AAOI and SOI to determine the connections among the four oscillations (Fig. 4). We allowed a maximum lag of 48 months to cover the full period of 3–7 years.

The highest correlation between the NOI and SOI was not a simultaneous one, but appeared at the time when the SOI led the NOI by two months, as shown in previous findings (Fu and Ye, 1988; Jin and Chen, 1992). The maximum statistically significant negative lagged correlations were with the NO leading (lagging) the SO by 27 (22) months. This indicated that the time variations in the NO and SO presented a period of approximately 3–5 years, i.e., the NO coupled with the SO strongly in the 3–5-yr period.

The lagged correlation between the NO and NPO differed from that between the NO and SO. The maximum statistically significant positive correlation was with the NPO leading the NO by 15 months, and the maximum statistically significant negative correlation was with the NPO lagging the NO by 12 months. These results suggested that the NO^- (NO^+) led the NPO^+ (NPO^-) by approximately 12 months, and the NPO^+ (NPO^-) led the NO^+ (NO^-) by approximately 15 months. This process took approximately 27 months from the NO^+ (NO^-) → NPO^- (NPO^+) → NO^- (NO^+). The whole process took approximately 54 months, being identical with the period of the so-called EN/LN cycle. These results are consistent with previous case studies (Wu and Chen, 1995).

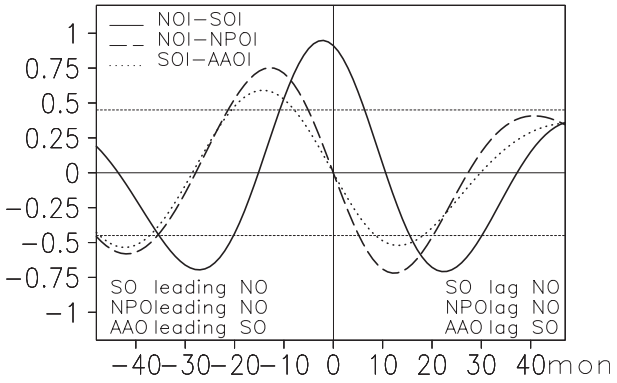

Fig. 4. Lagged correlation between the NO and SO (solid line), the NO and NPO (dashed line), the SO and AAO (dotted line), and the 95% confidence level (horizontal dashed line). The oscillation indices are replaced by corresponding PCs.

The lagged correlation between the SO and AAO was similar to that between the NO and NPO. The maximum positive (negative) correlation was with the AAO leading (lagging) the SO by 14 (13) months. This explained why the contemporaneous correlation between the SO and AAO was very weak. The whole process also lasted approximately 54 months from the SO^- (SO^+) → AAO^+ (AAO^-) → SO^+ (SO^-), and again from the SO^+ (SO^-) → AAO^- (AAO^+) → SO^- (SO^+).

4.2. *The evolution of circulation during the transition chains of the four oscillations*

Figure 5 shows the sequence of lag correlation fields of the NOI and SLPAs, with maximum lags of 30 months, to study the evolution of SLPAs during the transitions. Here, they are given at intervals of 6 months. We defined the NO leading SLP at 30 months as month −30, the zero-lag as month 0, and the NO lagging SLP at 30 months as month +30. The characteristics of circulation evolution revealed by different oscillation indices were similar to each other, differing only by a time delay.

At month −30, the negative SLP correlations occurred in the eastern equatorial Pacific basin, and the positive SLP correlations occupied the rest of the tropical area, including the western equatorial Pacific and the tropical Indian Ocean. The SLP correlations displayed a classic NO^- and SO^- structure. There were quasi-stationary Rossby wave trains from the eastern Pacific to the middle and high latitudes following a large circular route in the North and South Pacific that yielded the Pacific–North American pattern (Wallace and Gutzler, 1981) and the Pacific–South American pattern (Cai and Baines, 2001).

In the next one and a half years (month −30 to −12), the negative SLP correlations in the tropics propagated eastwardly from the western Pacific to the middle Pacific. Meanwhile, the positive SLP correlations in the eastern Pacific split into two parts: one moving eastward into the tropical Atlantic Ocean, and the other moving northwestward along the western shore of North America and reaching the Aleutians.

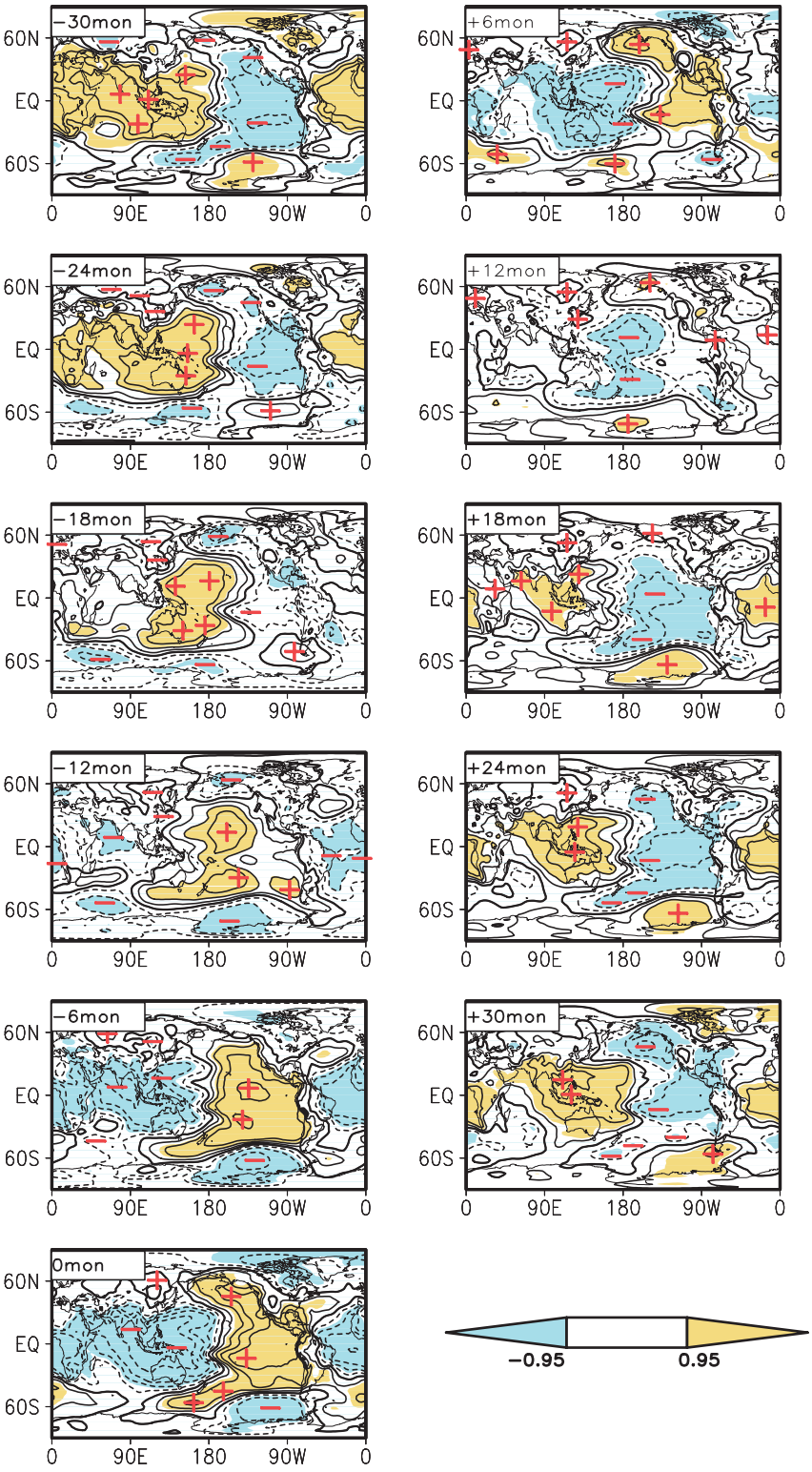

Fig. 5. The distribution of cross correlation between the interannual NOI (NPC1) and interannual SLPAs during 1951–2006 with a maximum 30-month lag. Shaded areas indicate correlations that are significant at the 95% confidence level. The contour interval is 0.15. Solid lines represent positive values; dashed lines represent negative values. The thick solid line is the zero line, while the plus symbols represent the centers of positive correlation and the minus symbols the centers of negative correlation.

The NO^- transitioned into the NPO^+ approximately at month -12. Due to the open oceans in the Southern Hemisphere, the positive and negative SLP correlations displaced sequentially eastwardly and encircled the globe. From month -30 to -12, the positive SLP correlations in the southeastern Pacific near the Drake Strait moved into the southern Atlantic Ocean, and the negative SLP correlations in the southwestern Pacific displaced into the Ross Sea and enhanced the meridional SLP gradients in the southern Pacific. The SO^- transitioned into the AAO^+. These characteristics of the evolution of interannual SLPs in both hemispheres are consistent with previous observations and modeling studies (Lau and Nath, 1994; Peterson and White, 1998; White and Cayan, 2000; Ribera and Mann, 2002, 2003).

During month -12 to 0, the positive SLP correlations in the subtropical middle Pacific moved eastward, reached the eastern Pacific and increased strongly. Meanwhile, the negative SLP correlations from the tropical Indian Ocean and from the middle latitudes of Asia moved into the western Pacific warm pool and strengthened. The zonal gradients of SLP in the tropical Pacific Ocean increased, and the NO^+ and the SO^+ were prominent.

Tracing the negative SLP correlations in the tropical Indian Ocean revealed their four origins: (1) the middle latitudes of Asia (A in Fig. 6), from where the SLP correlations propagated southeastward into the western Pacific warm pool; (2) the tropical Atlantic Ocean (B in Fig. 6), from where the SLP correlations propagated eastward across Africa to the Indian Ocean; (3) the Southwest Indian Ocean (C in Fig. 6), from where the correlations propagated northeastward across the Indian Ocean from high latitudes to the tropics; and (4) the North Atlantic Ocean and Northern Europe (D in Fig. 6), from where the correlations propagated southeastward across Europe.

From month 0 to $+30$, a similar evolution of SLP correlations appeared, albeit with the opposite sign. The NO^+ (SO^+) transitioned to the NPO^- (AAO^-) at approximately month $+18$, and the NPO^- (AAO^-) to the NO^- (SO^-) at approximately month $+24$ to $+30$.

The results described above were based on the oscillations represented by PCs. The cross-lag-correlations of the observed oscillation indices against SLP (not shown) resembled those in Figs. 4 and 5.

POP analysis is used widely to extract information on spatial propagating modes (von Storch et al., 1995; Tang, 1995). In the present study, POP analysis was applied to the interannual variations in SLPAs over the Pacific basin (75°S–75°N, 90°E–90°W). An EOF expansion was first performed, and only the first four EOF time series were retained, which explained 74.0% of the total variance. The decay time of the first POP mode (POP1) was the longest (458.39 months). Its period was 62.91 months, which was roughly the period of the four oscillation transition cycles obtained by the cross-time-lag correlation analysis. The POP1 coefficients explained 71.31% of the variance, so they contained $74.0\% \times 71.31\% = 54.25\%$ of the total variance in the interannual SLPA data. The real and imaginary parts of the spatial distribution of POP1 and its coefficients are shown in Fig. 7. The pattern of the real part of POP1 (top left of Fig. 7) reflected the out-of-phase variations in SLPAs between the subtropics and the mid-latitudes, and resembled the structures of the NPO^- and AAO^-. The pattern of the imaginary part of POP1 (top right of Fig. 7) reflected the east–west oscillations in the tropics, and resembled the structures of NO^- and SO^-. The time series of the POP coefficients oscillated regularly (Fig. 7, bottom row). The POP patterns appeared in sequence [$\ldots \rightarrow NPO^-$ (AAO^-) $\rightarrow NO^-$ (SO^-) $\rightarrow NPO^+$ (AAO^+) $\rightarrow NO^+$ (SO^+) $\rightarrow NPO^-$ (AAO^-) $\rightarrow \ldots$] and the transition chains of the four oscillations and their periods revealed by the POP method were similar to those obtained through the cross-time-lag correlation analysis.

Thus, the empirical analysis provided distinct evidence of the eastward propagation of alternate positive/negative SLPAs in the North and South Pacific, leading to a complete transition chain ($NO^- \rightarrow NPO^+ \rightarrow NO^+ \rightarrow NPO^- \rightarrow NO^-$ and $SO^- \rightarrow AAO^+ \rightarrow SO^+ \rightarrow AAO^- \rightarrow SO^-$) in 4–6 years. The travelling paths of the interannual SLPAs are drawn schematically in Fig. 6.

4.3. *Characteristics of the transitions*

The characteristics of the transition chains of the four oscillations was studied by their trajectories in 2D phase space of the North and South Pacific spanned by NPC1 and NPC2 and by SPC1 and SPC2, respectively (Fig. 8). The phase images indicate the characteristics of the transition chains of the four oscillations to be as follows:

(1) Periodicity. The trajectory rotated around its center in the phase space, and represented the transition chains among the four oscillations. There were 11 nearly closed cycles in both phase spaces, with two unclosed ones: one from 1951 to 1953, and the other from the summer of 2004 to the end of 2006. The beginning and end of each closed cycle are shown

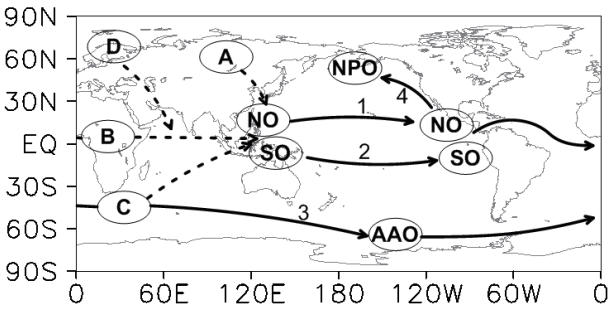

Fig. 6. Illustration of the global circuit linking the four oscillations. The solid line (line 1 and 2) in the tropics delineates the path of the SLPAs as they propagate eastward across the Pacific basin. Lines 3 and 4 delineate the path of the SLPAs propagating eastward around the globe in the Southern Ocean and propagating northwestward from the eastern Pacific to the Aleutian area, respectively. The dashed lines delineate the path of the SLPAs propagating into the western Pacific warm pool from the mid-latitudes of Asia (A), the tropical Atlantic Ocean (B), the southwestern Indian Ocean (C), and Northern Europe (D).

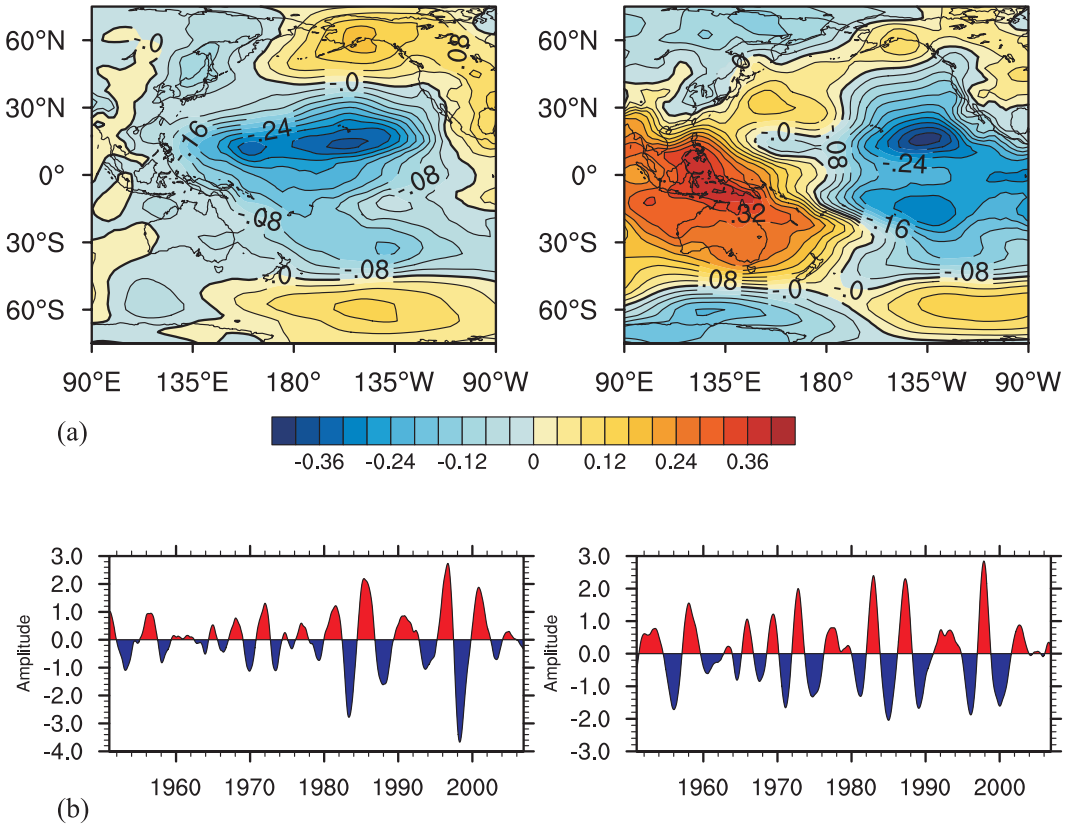

Fig. 7. (a) The patterns and (b) the coefficient time series of the real (left) and imaginary (right) parts of POP1.

Table 2. The beginning and end times and the type of each transition chain between the NO and NPO and the SO and AAO. The durations of each cycle are also shown (units: yr).

	NO-NPO			South Pacific		
	Time	Duration	Type	Time	Duration	Type
1	Jan 1955–Jan 1961	5.08	T	Jan 1954–Apr 1959	5.33	E
2	Feb 1961–Apr 1964	3.25	E	May 1959–Jul 1964	5.25	T
3	May 1964–Mar 1967	2.92	T	Aug 1964–May 1968	3.75	E
4	Apr 1967–Aug 1971	4.33	E	Jun 1968–Aug 1971	3.25	E
5	Sep 1971–Jan 1975	3.42	E	Sep 1971–Jan 1975	3.42	E
6	Feb 1975–Dec 1980	5.92	T	Feb 1975–Dec 1980	5.92	T
7	Jan 1981–Jan 1985	4.08	E	Jan 1981–Dec 1984	4.00	T
8	Feb 1985–Jan 1989	4.00	E	Jan 1985–Jan 1989	4.08	E
9	Feb 1989–May 1995	6.33	E	Feb 1989–Apr 1995	6.25	E
10	Jun 1995–Aug 1999	4.25	E	May 1995–Apr 2000	5.00	E
11	Sep 1999–Apr 2004	4.67	E	May 2000–Apr 2004	4.00	E
Average		4.38			4.57	

Note: E, elliptical orbit; T, two-bladed orbit.

in Table 2. The shortest transition chain in the North Pacific occurred from May 1964 to March 1967, and lasted for 35 months. The shortest one in the South Pacific was from June 1968 to August 1971, and lasted for 39 months. The longest cycle in the North and South Pacific spanned from approximately February 1989 to May 1995, and lasted for 76 and 75 months, respectively. The average period of one transition chain in the North Pacific was 4.38 years, while it was 4.57 years in the South Pacific. Eight of the 11 transition chains in both the North and South Pacific lasted for 4–6 years.

(2) Synchrony. Although the phase spaces were constructed independently, the time of the beginning and end of each transition chain of the North and South Pacific were nearly the same, especially after the 1970s. This was consistent with synchronous variations in the NO and the SO (Fu and Ye, 1988).

(3) Multiple types. There were two types of orbits. Most orbits (eight of 11 cycles, Table 2) in either the North or South

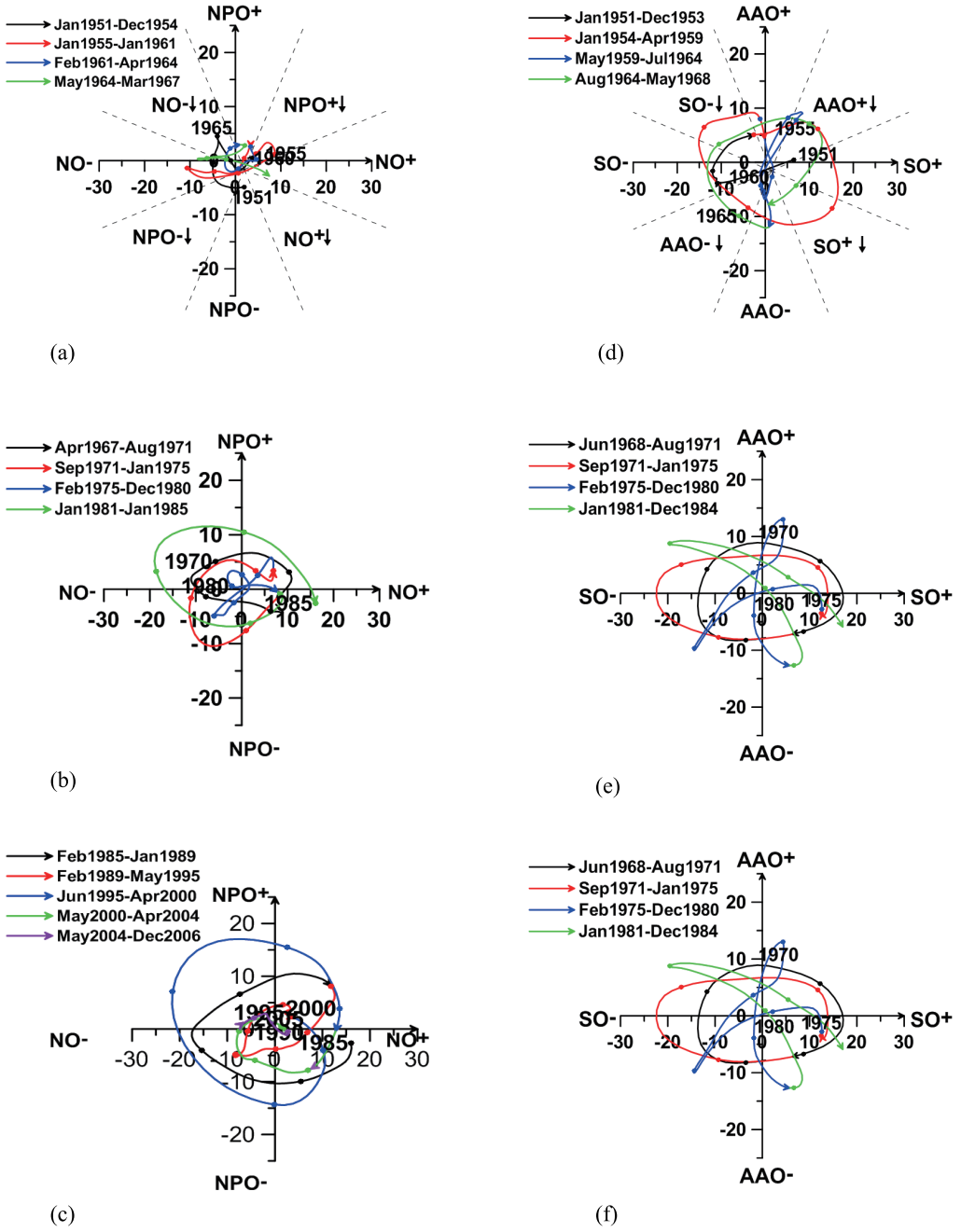

Fig. 8. (Left) 2D phase portrait in the plane spanned by NPC1 and NPC2: (a) from Jan 1951 to Mar 1967; (b) from Apr 1967 to Jan 1985; and (c) from Feb 1985 to Dec 2006 (bottom). (Right) The same as (left) but by SPC1 and SPC2: (d) from Jan 1951 to May 1968; (e) from Jun 1968 to Dec 1984; and (f) from Jan 1985 to Dec 2006. The numbers represent years. The dashed lines in (a) are the positions representing eight typical phases of the transition chain of the four oscillations. Four transition phases are denoted by the down arrow (↓). For example, $NO^+ \downarrow$ represents the transition phase from NO^+ to NPO^-.

Pacific were elliptical. For the elliptical orbits, the differences between the amplitudes of the NO and the NPO, or the SO and the AAO, were small. The phase points travelled through the four quadrants and displayed a regular motion in physical space. We divided the entire transition chains of the four oscillations into eight phases, as shown in Fig. 8a. The composite phases in physical space (Fig. 9) were similar to the results from the cross-time-lag correlation analysis.

Another type was the two-bladed orbit, whose amplitudes of the NO (SO) were larger than those for the NPO (AAO). The two-bladed orbits corresponded to the standing mode in the evolution of SLPAs during the transition. For example, from February 1975 to December 1980, the meridional SLP gradients in the North and South Pacific were weak (not

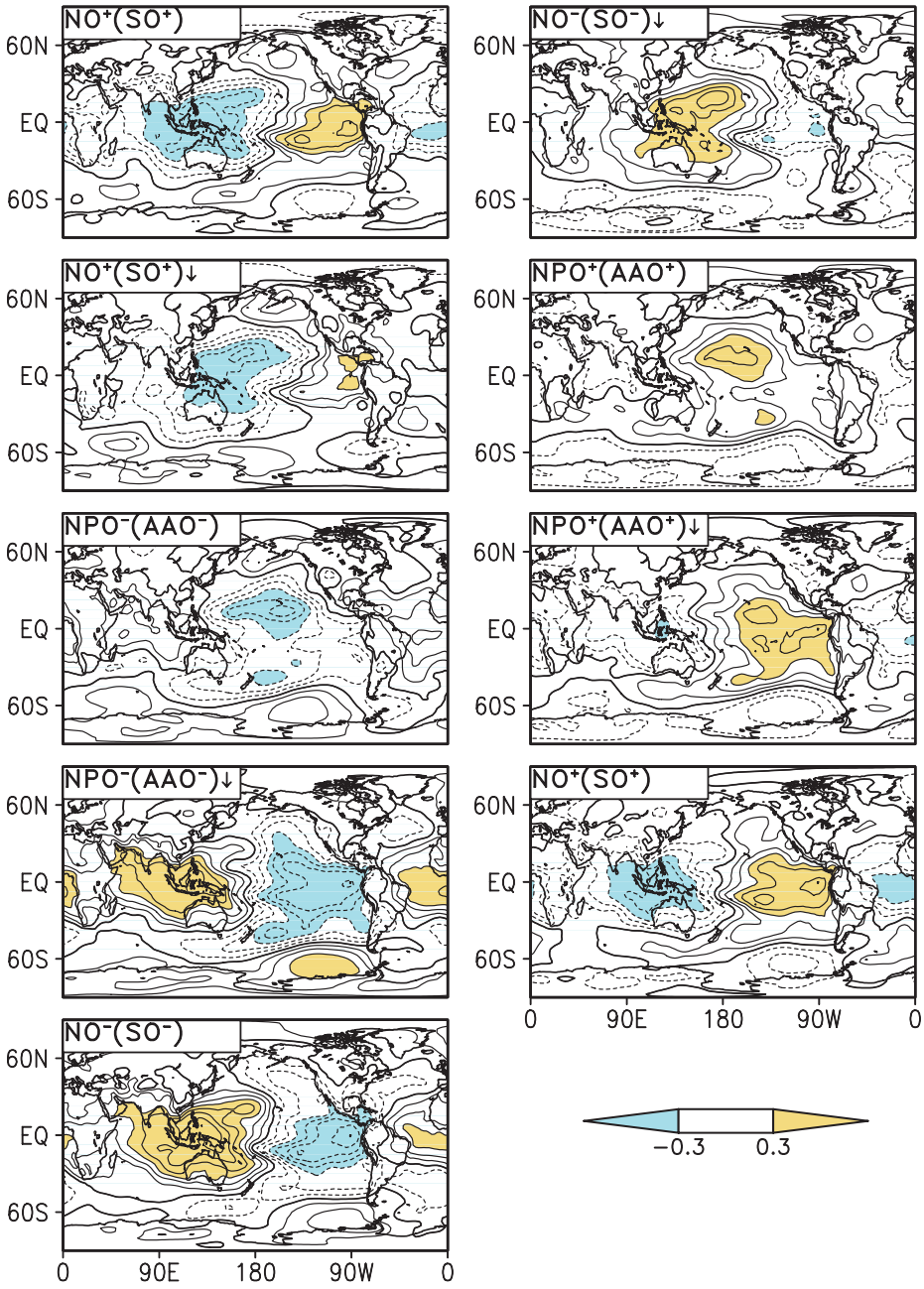

Fig. 9. Composites of monthly SLPAs associated with the eight typical phases of the transition chains of the four oscillations indicated in Fig. 7. Interval: 0.1.

shown). The transitions between the positive and negative SLPAs over the tropical Pacific were fast, and thus the amplitudes of the NPO and AAO were much weaker than those of the NO and SO.

The results of the empirical analysis and the phase space analysis showed that the general pattern of the transition chains of the four oscillations was the elliptical orbit, which corresponded to the travelling wave mode of the interannual variation in SLPAs over the Pacific Ocean. The eastward propagation of alternate positive/negative SLPAs was distinctly evident during the transition chains of the four oscillations as $NO^- \rightarrow NPO^+ \rightarrow NO^+ \rightarrow NPO^- \rightarrow NO^-$ or $SO^- \rightarrow AAO^+ \rightarrow SO^+ \rightarrow AAO^- \rightarrow SO^-$ in 4–6 years.

5. Discussion and conclusions

The present reported study investigated the connections and transition chains of four major oscillations (the NO, SO, NPO and AAO) on the interannual scale. The main results can be summarized as follows:

(1) The leading modes of the interannual variations in the low-level circulation over the North and South Pacific were the NO and SO, reflecting the oscillations between the eastern and western Pacific. The second leading modes were the

NPO and AAO, which reflected the oscillations between the subtropics and the high and middle latitudes.

(2) The four oscillations were found to be closely connected. In general, the transition chains of the four oscillations followed the pattern $NO^- \rightarrow NPO^+ \rightarrow NO^+ \rightarrow NPO^- \rightarrow NO^-$ or $SO^- \rightarrow AAO^+ \rightarrow SO^+ \rightarrow AAO^- \rightarrow SO^-$. The beginning and end of the transition chains of the oscillations in the North and South Pacific were roughly simultaneous, especially after the 1970s. The period of transition was approximately 4–6 years.

(3) The eastward propagation of alternate positive/negative SLPAs was distinctly evident during the transition chains of the four oscillations. The eastward propagation of SLPAs along the tropical Pacific, and the northwestward propagation of SLPAs from the eastern Pacific toward the Aleutian region, led to the transition between the NO and NPO. The SLPAs in the middle and high latitudes of the South Pacific that were out-of-phase with those in the tropical Pacific Ocean also propagated eastward, resulting in the transition between the SO and AAO. Figure 6 summarized the travel paths of the SLPAs over the Pacific Basin.

The SO was originally identified as a stationary oscillation of SLPA between the eastern and western Pacific. Then, later, the interannual SLPAs propagating eastward were discovered (Krishnamurti et al., 1986; Yasunari, 1987). These significant anomalies of SLP originate from Central Asia or Eurasia, then move to the Indian Ocean (Barnett, 1985). The propagation of SLPAs in the North Pacific was also observed (Chen and Fan, 1994). The propagation of SLPAs is the result of the air–sea interaction cycle. During an EN event, the positive air temperature anomalies in the tropics are approximately 1–1.5 standard deviations due to enhanced heat fluxes from the middle and eastern Pacific. The negative temperature anomalies locate over the mid- and high-latitude areas, and the increased meridional gradient of temperature favors the development of zonal circulation there. Furthermore, enhanced Hadley circulation in both hemispheres leads to more angular momentum transportation from the tropics to the middle latitudes and an additional enhancement of zonal circulation. Meanwhile, weakened Walker circulation leads to anomalous easterlies and the so-called "cross-equatorial tropical anticyclone pairs" to prevail over the western Pacific, which are components of the NO and SO. During the mature phase of EN, zonal circulation prevails over mid- and high-latitude areas, and the cross-equatorial tropical anticyclone pairs occupy the western Pacific. As the EN transitions to LN, the zonal circulation in the middle and high latitudes transitions to meridional circulation and the Walker circulation is enhanced, resulting in a deepening of the Aleutian Low and an enhancement of the highs in the vicinity of the date line (Zong, 2007). On the other hand, the long-wavelength coastally-trapped waves excited by the equatorial Kelvin wave may lead to the northwestward propagation of the SLPAs from the eastern Pacific to the North Pacific (Enfield and Allen, 1980; Lyman and Johnson, 2008). The easterly anomalies in the tropical Pacific favor the advection of cold SSTAs from the western Pacific to the eastern Pacific. These cold SSTAs lead to anticyclonic anomalies in the east (Weisberg and Wang, 1997), and the subsequent eastward propagation of the anticyclone pairs could be due to an ocean–atmosphere coupling process between SSTAs and the overlying SLPAs (Tourre and White, 1997). When the anticyclone pairs arrive in the middle tropical Pacific, NO^- transitions to NPO^+. In the Southern Hemisphere, the paths of the travelling SLPAs in the Southern Hemisphere resemble Fig. 10 in White et al. (2002), which summarizes the feedback between the Antarctic Circumpolar Wave and the EN.

Thus, the transition chains of the four oscillations connected with the EN/LN cycle closely. Their connection is discussed in Part II of this paper, along with the presentation of a new statistical approach to predict EN/LN.

Acknowledgements. The authors are grateful to Prof. JI Liren, Prof. SUN Shuqing and the two anonymous reviewers for their constructive suggestions, which improved the manuscript substantially. This work was supported by the National Basic Research Program of China (Grant No. 2012CB957800) and the National Key Technologies R&D Program of China (Grant No. 2009BAC51B02).

REFERENCES

Barnett, T. P., 1985: Variations in near-global sea level pressure. *J. Atmos. Sci.*, **42**(5), 478–501.

Barnett, T. P., D. W. Pierce, M. Latif, D. Dommenget, and R. Saravanan, 1999: Interdecadal interactions between the tropics and midlatitudes in the Pacific basin. *Geophys. Res. Lett.*, **26**, 615–618.

Bjerknes, J., 1969: Atmospheric teleconnections from the equatorial Pacific. *Mon. Wea. Rev.*, **97**, 163–172.

Cai, W. J., and P. G. Baines, 2001: Forcing of the Antarctic circumpolar wave by El Niño-Southern Oscillation teleconnections. *J. Geophys. Res.*, **106**, 9019–9038.

Carvalho, L. M. V., C. Jones, and T. Ambrizzi, 2005: Opposite phases of the Antarctic oscillation and relationships with intraseasonal to interannual activity in the tropics during the Austral Summer. *J. Climate*, **18**, 702–718.

Chen, L. T., 1982: Interaction between the subtropical high over the North Pacific and the sea surface temperature of the eastern equatorial Pacific. *Scientia Atmospherica Sinica*, **6**, 148–156.

Chen, L. T., 1992: The relationship between long-term variations in El Niño and the Northern Oscillation during the last 100 years. *Chinese Sci. Bull.*, **37**, 312–316.

Chen, L. T., and B. L. Yan, 1989: The EOF analysis of sea level pressure in the North Pacific related to the Northern Oscillation. *Chinese J. Atmos. Sci.*, **13**, 38–43. (in Chinese)

Chen, L. T., and Z. Q. Zhan, 1984: Teleconnection of pressure anomalies between the eastern and western North Pacific. *Chinese Sci. Bull.*, **29**, 642–645.

Chen, L. T., and Z. Fan. 1994: On 3.5-year coupled oscillation between Northern Oscillation and sea surface temperature of the Equatorial Pacific. *Journal of Nanjing University*, Special Issue, 158–166.

Enfield, D. B., and J. S. Allen, 1980: On the structure and dynamics of monthly mean sea level anomalies along the pacific coast of North and South America. *J. Phys. Oceanogr.*,

10, 557–578.

Fu, C. B., and D. Z. Ye, 1988: The tropical very low-frequency oscillation on interannual scale. *Adv. Atmos. Sci.*, **5**, 369–388.

Gong, D. Y., and S. W. Wang, 1999: Definition of Antarctic oscillation index. *Geophys. Res. Lett.*, **26**, 459–462.

Jin, F. F., 1997: An equatorial ocean recharge paradigm for ENSO. Part I: Conceptual model. *J. Atmos. Sci.*, **54**, 811–829.

Jin, Z. H., and L. T. Chen, 1992: A comparative study on relationship of the Southern and the Northern Oscillations with the sea surface temperature in the Pacific Ocean. *Acta Oceanologica Sinica*, **14**, 19–27. (in Chinese).

Kalnay, E., and Coauthors, 1996: The NCEP/NCAR 40-year reanalysis project. *Bull. Amer. Meteor. Soc.*, **77**, 437–471.

Krishnamurti, T. N., S. H. Chu, and W. Iglesias, 1986: On the sea level pressure of the Southern Oscillation. *Arch. Meteor. Geophys. Bioclimatol.* (*Ser. A*), **34**, 385–425.

Lau, N. C., and M. J. Nath, 1994: A modeling study of the relative roles of tropical and extratropical SST anomalies in the variability of the global atmosphere-ocean system. *J. Climate*, **7**, 1184–1207.

Li, C. Y., 1990: Interaction between anomalous winter monsoon in East Asia and El Nino Events. *Adv. Atmos. Sci.*, **7**(1), 36–46.

Li, C. Y., 1991: *Low-Frequency Oscillation in the Atmosphere*. China Meteorological Press, Beijing, 207 pp. (in Chinese)

Livezey, R. E., and W. Y. Chen, 1983: Statistical field significance and its determination by Monte Carlo techniques. *Mon. Wea. Rev.*, **11**, 46–59.

Lorenz, E. N., 1963: Deterministic nonperiodic flow. *J. Atmos. Sci.*, **20**, 130–141.

Lyman, J. M., and G. C. Johnson, 2008: Equatorial Kelvin wave influences may reach the Bering Sea during 2002 to 2005. *Geophys. Res. Lett.*, **35**, L14607, doi: 10.1029/2008GL034761

Montgomery, R. B., 1940: Report on the work of G. T. Walker. *Mon. Wea. Rev.*, **39**, 1–22.

Peng, J. B., Q. Y. Zhang, and L. T. Chen, 2011: Connections between different types of El Niño and Southern/Northern Oscillation. *Acta Meteorologica Sinica*, **25**, 506–516.

Peng, J. B., L. T. Chen, and Q. Y. Zhang, 2013: The relationship between the El Niño/La Niña cycle and the transition chains of four atmospheric oscillations and a new approach to the prediction of ENSO Events. Part II: the relationship and approach of prediction. *Adv. Atmos. Sci.*, doi: 10.1007/s00376-013-2279-9, accepted.

Peterson, R. G., and W. B. White, 1998: Slow oceanic teleconnections linking the Antarctic Circumpolar Wave with the tropical El Niño-Southern Oscillation. *J. Geophys. Res.*, **103**, 24 573–24 583.

Pierce, D. W., T. P. Barnett, and M. Latif, 2000: Connections between the Pacific Ocean Tropics and midlatitudes on decadal timescales. *J. Climate*, **13**, 1173–1194.

Raphael, M. N., and M. M. Holland, 2006: Twentieth century simulation of the southern hemisphere climate in coupled models. Part 1: Large scale circulation variability. *Climate Dyn.*, **26**, 217–228.

Rasmusson, E. M., and T. H. Carpenter, 1982: Variations in tropical sea surface temperature and surface wind fields associated with the Southern Oscillation-El Niño. *Mon. Wea. Rev.*, **110**, 354–384.

Ribera, P., and M. E. Mann, 2002: Interannual variability in the NCEP Reanalysis 1948–1999. *Geophys. Res. Lett.*, **29**, 132-1–132-4.

Ribera, P., and M. E. Mann, 2003: ENSO related variability in the Southern Hemisphere, 1948–2000. *Geophys. Res. Lett.*, **30**, 6-1–6-4.

Schneider, D. P., and E. J. Steig, 2002: Spatial and temporal variability of Antarctic ice sheet microwave brightness temperatures. *Geophys. Res. Lett.*, **29**, 25-1–25-4.

Schwing, F. B., T. Murphree, and P. M. Green, 2002: The Northern Oscillation Index (NOI): A new climate index for the northeast Pacific. *Progress in Oceanography*, **53**, 115–139.

Shi, N., F. Y. Wei, G. L. Feng, and T. L. Sheng, 1997: Monte Carlo test used in correlation and composite analysis of meteorological fields. *Journal of Nanjing Institute of Meteorology*, **20**, 355–359. (in Chinese)

Suarez, M. J., and P. S. Schopf, 1988: A delayed action oscillator for ENSO. *J. Atmos. Sci.*, **45**, 3283–3287.

Tang, B. Y., 1995: Periods of linear development of the ENSO cycle and POP forecast experiments. *J. Climate*, **8**, 682–691.

Tourre, Y. M., and W. B. White, 1997: Evolution of the ENSO signal over the Indo-Pacific domain. *J. Phys. Oceanogr.*, **27**, 683–696.

Vimont, D. J., D. S. Battisti, and A. C. Hirst, 2001: Footprinting: A seasonal connection between the tropics and mid-latitudes. *Geophys. Res. Lett.*, **28**, 3923–3926.

Vimont, D. J., J. M. Wallace, and D. S. Battisti, 2003: The seasonal footprinting mechanism in the Pacific: Implications for ENSO. *J. Climate*, **16**, 2668–2675.

von Storch, H., G. Bürger, R. Schnur, and J.-S. von Storch, 1995: Principal oscillation patterns: A review. *J. Climate*, **8**, 377–400.

Wallace, J. M., and D. S. Gutzler, 1981: Teleconnections in the geopotential height field during the Northern Hemisphere winter. *Mon. Wea. Rev.*, **109**, 784–812.

Wang, B., 1995: Interdecadal changes in El Niño onset in the last four decades. *J. Climate*, **8**, 267–285.

Wang, R. S., and B. Wang, 2000: Phase space representation and characteristics of El Niño-La Niña. *J. Atmos. Sci.*, **57**, 3315–3333.

Weisberg, R. H., and C. Wang, 1997: Slow variability in the equatorial West-Central Pacific in relation to ENSO. *J. Climate*, **10**(8), 1998–2017.

White, W. B., and D. R. Cayan, 2000: A global El Niño-Southern oscillation wave in surface temperature and pressure and its interdecadal modulation from 1900 to 1997. *J. Geophys. Res.*, **105**, 11 223–11 242.

White, W. B., S. C. Chen, R. J. Allan, and R. C. Stone, 2002: Positive feedbacks between the Antarctic Circumpolar wave and the global El Niño-Southern Oscillation Wave. *J. Geophys. Res.*, **107**, 29-1–29-17.

Wu, R. G., and L. T. Chen, 1995: 3–5 year time scale evolution of global 1000 hPa height anomaly during 1980–1989. *Chinese J. Atmos. Sci.*, **19**, 575–585. (in Chinese)

Yasunari, T., 1987: Global structure of the El Niño/southern Oscillation Part II: Time evolution. *J. Meteor. Soc. Japan*, **65**, 81–102.

Zeng, Q. C., 1987: The numerical simulation of climate (abstract). *Advances in Earth Science*, **2**, 19–22. (in Chinese).

Zhu, Y. L., and H. J. Wang, 2010: The Arctic and Antarctic oscillations in the IPCC AR4 coupled models. *Acta Meteorologica Sinica*, **24**(2), 176–188.

Zong, H. F., 2007: Study of impact process of global and local atmosphere anomaly caused by ENSO on precipitation during the Meiyu period. PhD dissertation, Institute of Atmospheric Physics, 109 pp.